Available online at www.sciencedirect.com
ScienceDirect
Journal of Power Sources 176 (2008) 373–380
JOURNAL OF POWER SOURCES
www.elsevier.com/locate/jpowsour

An innovative computational algorithm for simulation of lead-acid batteries

Vahid Esfahanian *, Farschad Torabi, Ali Mosahebi

Vehicle, Fuel and Environment Research Institute, Faculty of Mechanical Engineering, University College of Engineering, University of Tehran, Iran

Received 23 July 2007; received in revised form 11 October 2007; accepted 14 October 2007
Available online 24 October 2007

Abstract

Predicting transient behavior of lead-acid batteries during charge and discharge processes is an important factor in many applications including hybrid electric vehicles (HEVs). The conventional mathematical models, which are used to predict the battery dynamics, are either inaccurate or time-consuming. In this study, an improved and efficient mathematical model for simulation of flooded lead-acid batteries based on Computational Fluid Dynamics (CFD) and Equivalent Circuit Model (ECM) has been introduced which inherits the accuracy of CFD model and the physical understanding of ECM. This approach makes the numerical procedure very efficient and easy to implement. Moreover, because of simplification of boundary conditions (BC's), it is very fast which makes it quite suitable for real-time simulations. The present approach is verified by previous CFD models and experimental data.

Keywords: Battery modeling; Electrical circuit model; Real-time application; Kirchhoff's laws; Numerical simulation

1. Introduction

The lead-acid batteries have been widely used as secondary sources of energy for almost 150 years. High specific energy, high-rate discharge capability, low cost in both manufacturing and recycling and finally high energy density are the most important characteristics of this kind of batteries resulting into their growing usage. On the other hand, current characteristics of lead-acid batteries are not optimum and should be optimized. In order to improve the performance of lead-acid batteries trial-and-error methods, usually based on experimental tests, have been used for many years. Experimental tests are very valuable but very costly and time-consuming; also many design parameters such as acid gradient distribution cannot be obtained experimentally. Although these tests can lead to better performance, they never result into the best choice. Because of these deficiencies, various mathematical models have been developed to predict the dynamic behavior of lead-acid batteries. These different mathematical models have been proposed for different purposes. Among them ECM and CFD methods are of great importance.

In ECM method, each phenomenon in battery is modeled by an electrical component such as resistance, capacitor, etc. Then the whole battery is modeled as a complete electrical circuit whose solution simulates the battery dynamic behavior. This type of modeling is fast enough for real-time simulation and accurate for some parameters. Traditionally, this type of modeling is normally used to obtain dynamic (time-dependent) parameters of battery and spatial distributed parameters such as acid concentration gradient across the cell width is not considered, however, one can use the model to obtain the spatial parameters as well. Moreover, to obtain the battery parameters, one should perform some experimental tests [1–3].

In CFD model, on the other hand, the governing equations of the battery dynamic are solved using advanced numerical techniques. Since these governing equations are solved with respect to time and space, all the physical time and space dependent properties such as acid concentration and potential distribution

* Corresponding author. Tel.: +98 21 88020741; fax: +98 21 88020741.
E-mail addresses: evahid@ut.ac.ir (V. Esfahanian), ftorabi@ut.ac.ir (F. Torabi), amosahebi@ut.ac.ir (A. Mosahebi).

0378-7753/$ – see front matter © 2007 Elsevier B.V. All rights reserved.
doi:10.1016/j.jpowsour.2007.10.052

Nomenclature

a	coefficient
A	specific electroactive area ($cm^2\ cm^{-3}$)
C	acid concentration ($mol\ cm^{-3}$)
D	diffusion coefficient ($cm^2\ S^{-1}$)
F	Faraday constant, 96,487 C mol^{-1}
i	current through liquid or solid ($A\ cm^{-2}$)
i_0	exchange current density
I	applied current ($A\ cm^{-2}$)
j	transfer current density ($A\ cm^{-2}$)
$\bar{j}$	mean transfer current density ($A\ cm^{-2}$)
J	transfer current ($A\ cm^{-2}$)
k	conductivity of liquid ($S\ cm^{-1}$)
L	Total width of a cell (cm)
Q	theoretical capacity (C cm−3)
R	resistance (S^{-1})
SoC	state of charge
t	time (s)
T	temperature (K)
ΔV	potential difference (V)
x	spatial dimension (cm)

Greek letters

α_a, α_c	anodic and cathodic transfer coefficient
ε	porosity
σ	conductivity of solid matrix ($S\ cm^{-1}$)
ϕ	electric potential (V)

Subscripts and superscripts

D	pertinent to diffusion
eff	effective, corrected for tortuosity
ex	exponent in the effective property
l	liquid phase
m	volume number
max	maximum
ref	reference
s	solid phase
0	initial value

across the cell can be obtained. Thus, such a modeling is able to give a very good understanding of battery parameters and detailed characteristic of battery dynamic, which makes it very suitable for design purposes.

Many efforts have been done in order to develop the appropriate set of governing equations for lead-acid batteries. Presence of the porous media and electrochemical reactions and being a multiphase system, lead to complexity of batteries nature. Neumann and Tiedmann [4] first developed a comprehensive porous electrode theory and applied it to simulate the discharge behavior of a lead-acid cell. Bernardi et al. [5] proposed a two-dimensional model to simulate the effects of the current collector tabs. Most recently, Wang and Gu [6] developed the mathematical governing equations of batteries which are obtained from the conservation laws. In their model, the effects of free convection have been considered and it was shown that fluid dynamics have a very important role in the batteries dynamic behavior. These equations can be used in all kinds of batteries (VRLA or vented lead-acid batteries) with little modification. Gu et al. [7] solved the governing equation of a lead-acid battery using a multiregion formulation. They used a set of boundary condition equations in the boundaries of each region (positive electrode/electrolyte, electrolyte/separator and so on) in order to interrelate the different regions of battery. The whole system was solved by a three-point finite difference scheme which results in a block tri-diagonal system of equations. But in order to maintain the second order of accuracy of the code, off diagonal elements appeared in their coefficient matrix. Hence, they used a modified bounded routine to solve the system. Gu et al. [8], on the other hand, introduced a set of governing equations which were valid in all cell regions. Therefore, it does not require any special system of equations for each region and their boundaries. They solved this system of equations by means of finite volume method (FVM). Esfahanian and Torabi [9] solved this system of equations using Keller-Box method. Their method has a second order accuracy in space as well as time. Since this method has a two-point algorithm and both functions and their derivatives are solved as unknowns, it is a very suitable method for solving the battery governing equations and does not require any special routine.

CFD models are very accurate but they suffer from being time-consuming. In CFD methods, a large nonlinear system of equations is solved iteratively. When the system is also stiff (like the system of equations in battery dynamic) its convergence is very slow and thus, it is very computationally expensive. Wang and Gu [6] reported that the solution of discharge and charge cycle using a one-dimension model required 10 s. While Esfahanian and Torabi [9] reported that 30 s is required to simulate the same cycle. It also worth noting that these simulations were based on flooded lead-acid batteries. Therefore, no side reaction such as hydrogen evolution or oxygen recycling was considered. Applying these phenomena to the simulations will increase the computational time in a very large amount. Moreover, extending the model to two or three dimension will increase the execution time considerably. These results show that in general, the CFD models may not be fast enough for real-time simulations, especially when the models are two and three-dimensional. Therefore, they cannot be used where the fast solution is required, i.e. in optimization or in real-time purposes like monitoring or real-time simulation of hybrid electric vehicle (HEV). Any method which can accelerate the CFD codes will be of great importance and interest.

In this study, a new innovative computational algorithm is introduced which is a combination of ECM and CFD methods. This model inherits the accuracy of CFD method (because the same governing equations are solved) and is fast like an ECM method. By this model, one can have an accurate result within a short time which makes this model very suitable for design as well as real-time purposes. The results of the present model are compared with previous CFD models, which showed the accuracy of code.

2. Mathematical model

A typical lead-acid cell is shown schematically in Fig. 1 which consists of the following regions: a lead-grid collector at $x=0$ which is at the center of the positive electrode; a positive PbO_2 electrode; an electrolyte reservoir; a porous separator; a negative Pb electrode; and finally a lead-grid collector at $x=l$ which is at the center of the negative electrode. The positive and negative electrodes consist of porous solid matrices whose pores are flooded by a binary sulfuric acid, H_2SO_4. The present model is assumed to be one-dimensional perpendicular to the faces of the electrodes.

During charge and discharge, the following electrochemical reactions occur:

- The positive electrode ($PbO_2/PbSO_4$):

$$PbO_{2(s)} + HSO_4^- + 3H^+ + 2e^- \underset{\text{Charge}}{\overset{\text{Discharge}}{\rightleftarrows}} PbSO_{4(s)} + 2H_2O \quad (1)$$

- The negative electrode ($Pb/PbSO_4$):

$$Pb_{(s)} + HSO_4^- \underset{\text{Charge}}{\overset{\text{Discharge}}{\rightleftarrows}} PbSO_{4(s)} + H^+ + 2e^- \quad (2)$$

In the present model, as an approximation, the effects of side reactions are neglected. Therefore, the model can be applied only on traditional vented lead-acid batteries. Side reactions, however, can be easily modeled with the same procedure.

2.1. Governing equations

As it was mentioned, the general governing equations of battery dynamic have been developed by Wang and Gu [6] which include all chemical and electrochemical reactions as well as the flow motion. In the present study, these equations are simplified for flooded lead-acid batteries.

Conservation of charge in solid and liquid phases is represented according to the following relations.

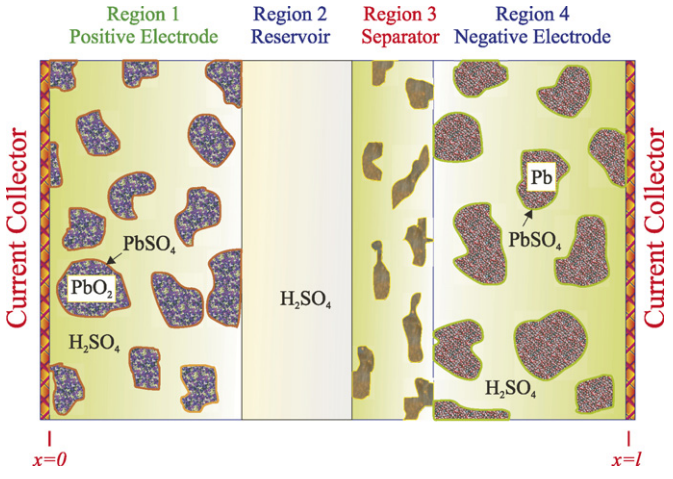

Fig. 1. Schematic illustration of a lead-acid cell.

Conservation of charge in solid:

$$\nabla(\sigma^{\text{eff}}\nabla\phi_s) - Aj = 0 \quad (3)$$

Conservation of charge in liquid:

$$\nabla(k^{\text{eff}}\nabla\phi_l) + \nabla(k_D^{\text{eff}}\nabla(\ln c)) + Aj = 0 \quad (4)$$

where j is the exchange current density (from solid phase to the electrolyte phase) and can be expressed in the general Butler-Volmer form:

$$j = i_0\left(\frac{c}{c_{\text{ref}}}\right)^{\gamma}\left\{\exp\left(\frac{\alpha_a F}{RT}\eta\right) - \exp\left(-\frac{\alpha_c F}{RT}\eta\right)\right\} \quad (5)$$

In this equation, the overpotential η is defined as $\eta = \phi_s - \phi_l - \Delta U_{PbO_2}$ for positive electrode and $\eta = \phi_s - \phi_l$ for negetive electrode, and ΔU_{PbO_2} is the open circuit potential.

Another conservation equation is obtained using a mass balance for ionic species in electrolyte phase, which is well known as the conservation of species equation. This equation in the case of one-dimensional modeling is simplified as

$$\frac{\partial(\varepsilon c)}{\partial t} = \nabla(D^{\text{eff}}\nabla c) + a_2\frac{Aj}{2F} \quad (6)$$

In the presence of electrochemical reactions, the porosity of the electrodes changes due to the volumetric change of the converted material. To account the porosity change of the electrodes, conservation of mass can be used. This balance results in

$$\frac{\partial\varepsilon}{\partial t} - a_1\frac{Aj}{2F} = 0 \quad (7)$$

The state of charge parameter (SoC) is defined as the ratio of instantaneous electrode capacity to the maximum theoretical capacity of electrode and thus can be evaluated by the following rate equation:

$$\frac{\partial(\text{SoC})}{\partial t} = \pm\frac{Aj}{Q_{\max}} \quad (8)$$

where, the positive and negative signs correspond to PbO_2 and Pb electrodes, respectively.

In Eqs. (3)–(8), the specific electroactive area A is a strong function of SoC and differs during charge and discharge because of different active materials involved. These areas can be related to the SoC via the following empirical relations [8]:

- Discharge:

$$A = A_{\max}\text{SoC}^{\zeta} \quad (9)$$

- Charge:

$$A = A_{\max}(1 - \text{SoC}^{\zeta}) \quad (10)$$

Details of the other governing equations and their coefficients which are functions of ε and SoC can be found in [7,8] and will not be repeated here. In this study, the main focus will be on conservation of charge and species equations (Eqs. (3), (4) and (6)).

2.2. Initial and boundary conditions

In order to solve the system of equations, initial and boundary conditions for primary variables are necessary. The initial condition for acid concentration is $c = c_0$. The appropriate BC's at $x = 0$ and $x = l$ for c and ϕ_l are $\partial c/\partial x = \partial \phi_l/\partial x = 0$; the BC's for potential in solid at $x = 0$ and $x = l$ are $-\sigma^{\text{eff}}(\partial \phi_l/\partial x) = I$ for a prescribed current density or $\phi_s = V$ at $x = l$ for a given voltage. It should be notice that at $x = 0$ potential in solid phase is assumed to be zero as a reference value ($\phi_s = 0$).

The transport equations for potentials in solid and liquid are elliptic partial differential equations (PDE). Mathematically, an elliptic PDE with Neumann type of BC's in all the boundaries of domain has a unique solution if: (a) it satisfies the compatibility equation and (b) at least one value is known inside the domain. Compatibility equation in the battery dynamic is interpreted as conservation of charge. It means that the amount of current that enters the cell at one electrode should leave the cell at the other electrode. To have a unique solution, one should specify a value for potential in one point; for example $\phi_s = 0$ at the center of the positive electrode. Then ϕ_l at the center of positive electrode can be obtained using compatibility equation [10]. All the potentials are calculated related to this reference potential. Without this reference point, a unique solution cannot be obtained.

3. Numerical difficulties

As it can be seen, the governing equations of battery are highly nonlinear and contain nonlinear source terms. Moreover, the system of equations is highly stiff and all equations are highly coupled together and elliptic in nature (require iterative methods to solve). But the most difficulties arise from Neumann-type BC's. Because of presence of this type of BC's, usual CFD techniques are very time-consuming and should be solved iteratively, especially for ϕ_l. As it mentioned both BC's of ϕ_l are Neumann type therefore, to obtain the solution, the value of ϕ_l should be assigned at one point and then with this guessed value the governing equations are solved. When the governing equations are solved, from the compatibility equation the value of ϕ_l should be modified. On the other hand, in the negative electrode, also there are two Neumann-type BC's for ϕ_s and similar to ϕ_l, the solution to its governing equation should be obtained iteratively using the compatibility equation. This procedure is highly time-consuming.

In this study, the conservation of charges in solid and liquid phase are used along with the compatibility equation through the whole domain to eliminate the iteration. Therefore, the solution will be faster.

4. Numerical scheme

The most time-consuming part of computation can be eliminated if the distribution of ϕ_s and ϕ_l are obtained by another mean. In the present study, a two-step scheme is introduced to overcome the problem. In the first step, the conservation of charge equations are considered (Eqs. (3) and (4)). Mathematically, these two couple equations have elliptic nature whose solutions require a lot of computational time. To reduce the computational time, these equations are combined by Kirchhoff's current and voltage laws (KCL and KVL) and are solved with an ECM based on finite volume method.

Using this new form of discretization, the distribution of ϕ_s and ϕ_l can be obtained much faster than the previous studies which were based on pure finite difference or finite volume methods. Once the distribution of ϕ_s and ϕ_l are obtained (at each time level), in the second step, the equation of conservation of species (6) is solved using Keller-Box method [9]. Since this equation is parabolic therefore, the solution can be found very quickly by marching in time. These two steps are considered in more detail in the next sections.

4.1. Step 1

In general, the applied current should be conserved throughout the cell. This current enters the cell from an external circuit and enters the solid phase. As it can be seen schematically in Fig. 2, the current enters the electrolyte through surface reactions whose rate is determined by kinetics of the reactions. At the end of the solid phase, all the current enters the electrolyte phase through which is carried by ions to the other electrode. On the other electrode surface, this current enters the solid phase again in a reverse manner.

As it described above, at each point inside the domain, two currents can be defined: current through solid phase (i_s) and current through liquid phase (i_l). Hence, the compatibility equation can be written at each point through the cell as

$$i_s + i_l = I_{\text{applied}} \tag{11}$$

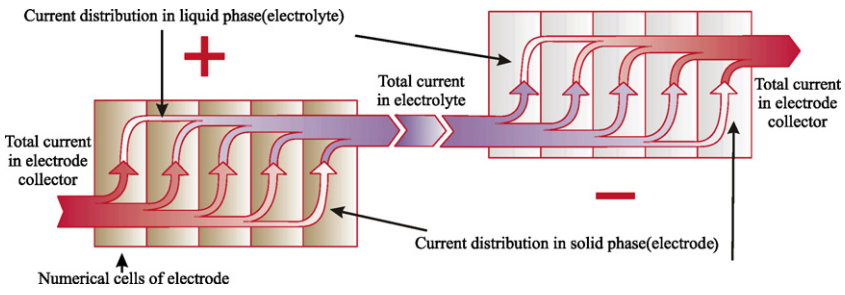

Fig. 2. Current distribution in solid and liquid phases.

Furthermore, conservation of charge implies:

$$\nabla i_s + \nabla i_l = \nabla I_{applied} = 0 \tag{12}$$

From Eqs. (3) and (4) conservation of charge equations in solid and liquid phases in one-dimension model can be rewritten as below

- Conservation of charge in solid phase:

$$\frac{\partial}{\partial x}\left(-\sigma^{eff}\frac{\partial \phi_s}{\partial x}\right) = -Aj \tag{13}$$

- Conservation of charge in liquid phase:

$$\frac{\partial}{\partial x}\left(-k^{eff}\frac{\partial \phi_l}{\partial x} - \frac{k_D^{eff}}{c}\frac{\partial c}{\partial x}\right) = +Aj \tag{14}$$

The currents through the solid and liquid phase are defined as

$$i_s = -\sigma^{eff}\frac{\partial \phi_s}{\partial x} \tag{15}$$

$$i_l = -k^{eff}\frac{\partial \phi_l}{\partial x} - \frac{k_D^{eff}}{c}\frac{\partial c}{\partial x} \tag{16}$$

Using these definitions in Eqs. (13) and (14) yield:

$$\frac{\partial (i_s)}{\partial x} = -Aj \tag{17}$$

$$\frac{\partial (i_l)}{\partial x} = Aj \tag{18}$$

In order to obtain the potentials in solid and electrolyte and exchange current between these two phases, each electrode is divided into a number of numerical cell or control volume (Fig. 2) over which all the parameters are assumed to be uniform and Eqs. (17) and (18) are integrated on each volume as follow:

- Current in solid phase at mth volume:

$$i_{s(m+1/2)} - i_{s(m-1/2)} = -A\bar{j}_m \Delta x_m = -J_m \tag{19}$$

- Current in liquid phase at mth volume:

$$i_{l(m+1/2)} - i_{l(m-1/2)} = A\bar{j}_m \Delta x_m = J_m \tag{20}$$

In Eqs. (19) and (20) $\bar{j}_{(m)}$ is the mean exchange current entered through the mth control volume from the solid phase to liquid phase or vice versa.

The electro-neutrality indicates that the sum of the current that enters a control volume must leave it, because no current is generated inside the volume. This fact can be denoted by summing up the two sides of Eqs. (19) and (20). Therefore, at each node the conservation of charge is satisfied automatically.

$$i_{s(m+1/2)} + i_{l(m+1/2)} = i_{s(m-1/2)} + i_{l(m-1/2)} = I_{applied} \tag{21}$$

It is observed that the exchange current J_m connects the currents through the solid and liquid phases; therefore each control volume can be modeled by an electric circuit which is shown in Fig. 3(a). As it can be seen, at the junction of solid surface of the electrode and electrolyte, a voltage difference exists which is known as overpotential. The surface overpotential is the driven potential which causes the current enters from the electrode to the electrolyte or vice versa. The amount of this current can be determined using Butler-Volmer equation (Eq. (5)).

From Eqs. (19) and (20), it is observed that these equations represent KCL in the electric circuit shown in Fig. 3(b) which express that the summation of all currents that enter a node should be zero. Also from KVL:

$$\begin{aligned}&(\phi_{s(m+1)} - \phi_{s(m)}) + (\phi_{l(m+1)} - \phi_{s(m+1)}) \\ &+(\phi_{l(m)} - \phi_{l(m+1)}) + (\phi_{s(m)} - \phi_{l(m)}) = 0\end{aligned} \tag{22}$$

Using this auxiliary equation eliminates the iteration on BC's required by pure CFD methods to satisfy the compatibility equation.

The currents in the solid and electrolyte can be obtained from improved Ohm's law. Eqs. (15) and (16) can be discretized to obtain the currents at the surfaces of mth control volume with second order of accuracy. For example at right surface of mth control volume:

$$\begin{aligned}i_{s(m+1/2)} &= -\sigma^{eff}\frac{\partial \phi_s}{\partial x}|_{(m+1/2)} \\ &= -\sigma^{eff}_{(m+1/2)}\frac{\phi_{s(m+1)} - \phi_{s(m)}}{\Delta x_{(m+1/2)}}\end{aligned} \tag{23}$$

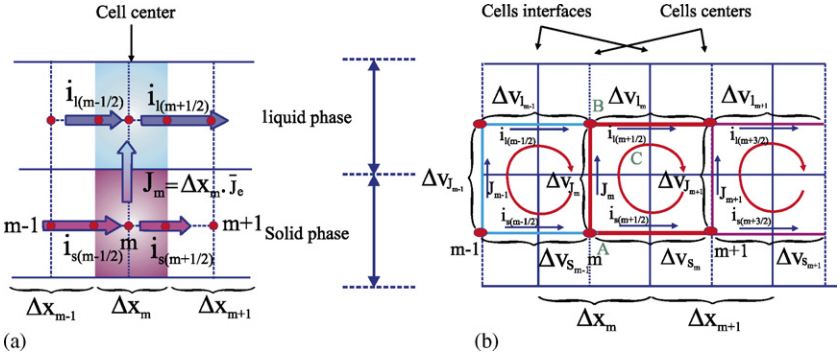

Fig. 3. Schematic illustration of (a) computational volume and (b) volume circuit model.

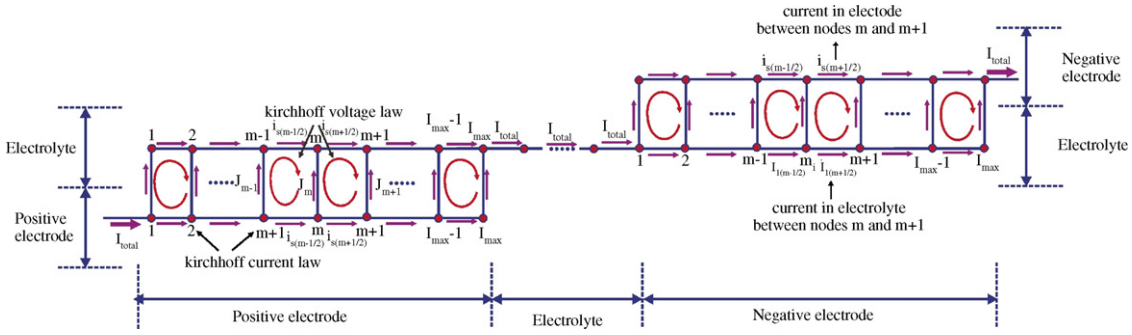

Fig. 4. Equivalent Circuit Model of the whole battery cell.

and

$$i_{l(m+1/2)} = -k^{\text{eff}}\frac{\partial \phi_l}{\partial x}|_{(m+1/2)} - \frac{k_D^{\text{eff}}}{c}\frac{\partial c}{\partial x}|_{(m+1/2)}$$
$$= -k_{(m+1/2)}\frac{\phi_{l(m+1)} - \phi_{l(m)}}{\Delta x_{(m+1/2)}} - \frac{k_D^{\text{eff}}}{c}\frac{\partial c}{\partial x}|_{(m+1/2)} \quad (24)$$

With the same order of accuracy[1], ohmic resistances $R_{s(m+1/2)} = (R_{s(m)} + R_{s(m+1)})/2$ and $R_{l(m+1/2)} = (R_{l(m)} + R_{l(m+1)})/2$ in which $R_{s(m)} = \Delta x_{(m)}/\sigma_{(m)}^{\text{eff}}$ and $R_{l(m)} = \Delta x_{(m)}/\sigma_{(m)}^{\text{eff}}$ are defined. Hence, Eqs. (23) and (24) can be rewritten as follow:

$$i_{s(m+1/2)} = -\frac{\phi_{s(m)} - \phi_{s(m+1)}}{R_{s(m+1/2)}} \quad (25)$$

$$i_{l(m+1/2)} = -\frac{\phi_{l(m)} - \phi_{l(m+1)}}{R_{l(m+1/2)}} - k_D\frac{1}{c}\frac{\partial c}{\partial x}|_{(m+1/2)} \quad (26)$$

Because the conservation of charge and species equations are solved uncoupled, the last term in Eq. (26) which determines the contribution of concentration gradient on i_l is considered as a source term and is known from the previous time step.

From Fig. 3, it is obvious that instead of the potential in nodes, the potential differences can be used to obtain the currents. Thus, three new variables are introduced:

$$\Delta V_{s(m)} = \phi_{s(m+1)} - \phi_{s(m)} \qquad \Delta V_{l(m)} = \phi_{l(m+1)} - \phi_{l(m)}$$
$$\Delta V_{J(m)} = \phi_{s(m)} - \phi_{l(m)} \quad (27)$$

Using these new variables Eq. (22) can be rewritten as

$$\Delta V_{s(m)} - \Delta V_{J(m+1)} - \Delta V_{l(m)} + \Delta V_{J(m)} = 0 \quad (28)$$

Finally, at each volume, there are three unknowns (Eq. (23)) and three equations (i.e. Eqs. (19), (20) and (28)) which should be solved to obtain the solution. In order to have a good accuracy, the whole battery is divided into a number of (namely n) volumes in series which will result a system of $3n$ unknowns and $3n$ equations (some of them neglected in the separator region). This model is illustrated in Fig. 4. Because J_m is a nonlinear function of $\Delta V_{J(m)}$ according to the Eq. (5), the system of equations should be linearized and solved iteratively. As indicated from Fig. 4 four Neumann-type BC's are reduced to only one Dirichlet-type BC which is at the current collector of positive electrode ($i_{s(1)} = I_{\text{applied}}$). Since the current at the other boundary is satisfied automatically ($i_{s(I_{\max})} = I_{\text{applied}}$), no boundary condition is required at the end of the equivalent circuit. After $\Delta V_{s(m)}$, $\Delta V_{l(m)}$ and $\Delta V_{J(m)}$ have been obtained, $\phi_{s(m)}$ and $\phi_{l(m)}$ can be computed using Eq. (27). It should be noted that at $x = 0$ the value of $\phi_{s(1)} = 0$ is used again as a reference.

4.2. Step 2

Once the distributions of ϕ_s and ϕ_l are found, one can obtain the acid concentration gradient (Eq. (6)) by solving numerically using Keller-Box method. The Keller-Box method and its application to battery modeling is explained in [9] and is not mentioned here again. After obtaining the battery parameters in this time step, the whole procedure is repeated again to advance to the next time step.

5. Results

The system of governing equations has been solved using this new combination of CFD and ECM method. To verify the above-mentioned procedure, the discharge, rest and charge problems of a lead-acid cell have been simulated. These samples have been studied by Gu et al. [7] and reproduced by Gu et al. [8] an Esfahanian and Torabi [9]. All the necessary parameters are the same as the ones used by Gu et al. [7].

Fig. 5 shows the simulated voltage of the battery cell versus time during discharge. The results of present study match very well with the results of the other researchers [7–9]. Charge behavior of the same cell is presented in Fig. 6 and is compared with the other studies [7,8]. In Fig. 7 the variations of acid concentration in time levels 0, 60 and 105 s are shown. The figure indicates that the results of present simulation agree with the previous studies [7–9]. As it can be seen, when the cell reaches cut-off voltage (i.e. $t = 105$ s), the acid is totally consumed in positive electrode. But in negative electrode, the acid is not totally consumed which means the negative electrode is over designed and can be optimized [11].

Fig. 8 shows the variation of charge across the electrodes at different time steps. The results show that during the battery discharge, the amount of charge in both electrodes decreases. But at the end of discharge, the electrodes still have a lot of charge which means these electrodes are not fully utilized.

[1] The averaging operator is second order.

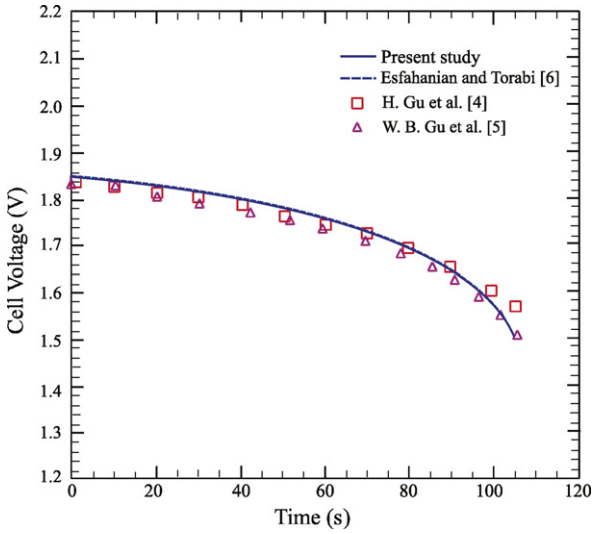

Fig. 5. Voltage of the cell during discharge.

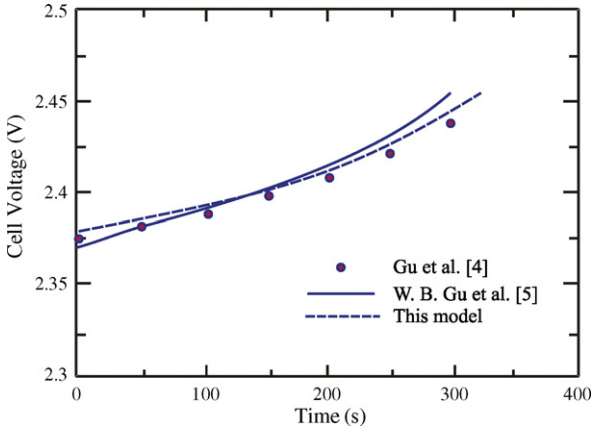

Fig. 6. Voltage of the cell during charge.

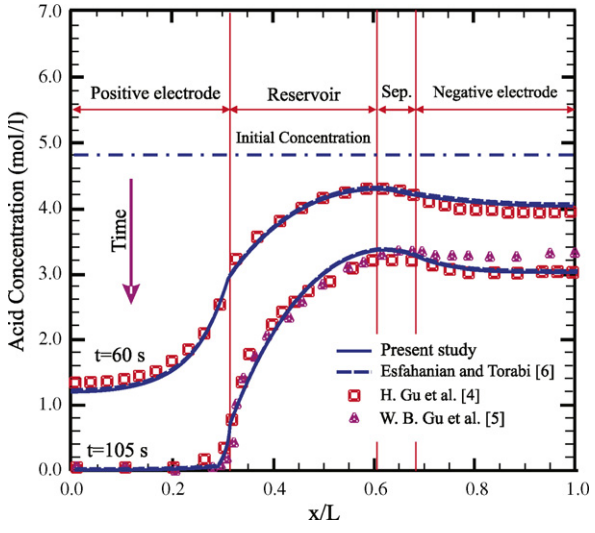

Fig. 7. Distribution of acid concentration across the cell width during discharge.

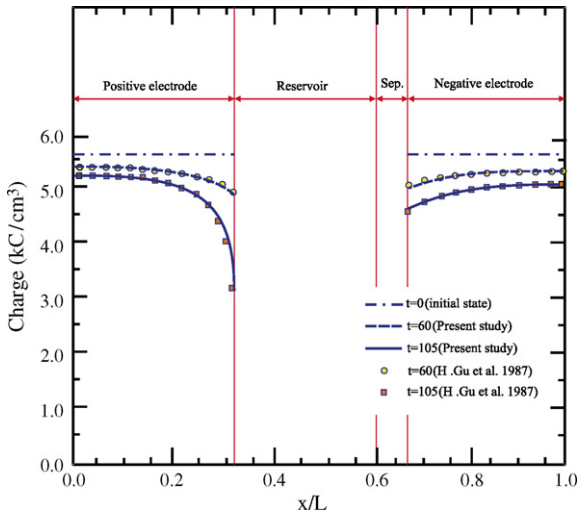

Fig. 8. Distribution of charge across the cell width during discharge.

In Fig. 9 the distribution of porosity throughout the cell in time levels 0, 60 and 105 s are presented. As it can be observed, because the converted materials occupy greater volume rather than initial ones, the electrodes holes gradually are filled during discharge hence, the electrodes porosity decreases.

In Fig. 10, the overpotential distributions of electrodes are presented. As it can be seen, during discharge there is a negative overpotential distribution throughout positive electrode and a positive distribution in negative electrode. Because the total internal resistance of the cell increases during discharge process, the magnitudes of these overpotentials increase to overcome this resistance.

Conservation of charge during charge and discharge are presented in Fig. 11. As it can be seen, through the width of one electrode, current enters the electrolyte. At the end of solid phase of that electrode, all the current has entered the electrolyte phase. On the other electrode surface, this current enters the solid phase

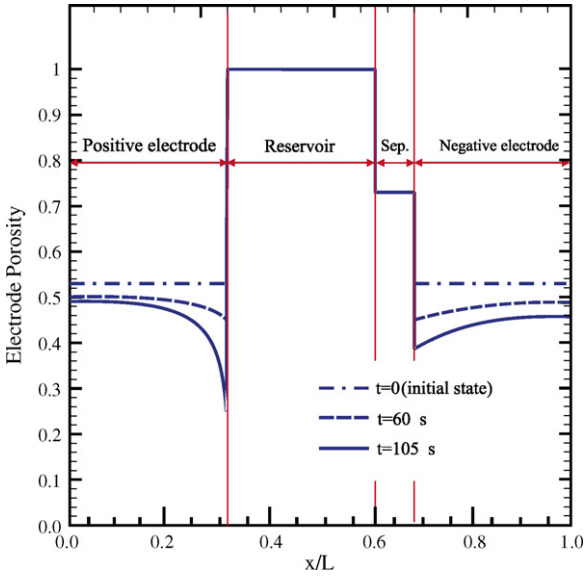

Fig. 9. Distribution of porosity across the cell width during discharge.

Table 1
Comparison of the needed CPU time between the new approach and the classical one

Total number of nodes N	Classical approach (s)	New approach (s)	Speed up factor
50	21.1	0.39	54.1
100	39.9	0.75	53.2
150	59.7	1.12	53.3

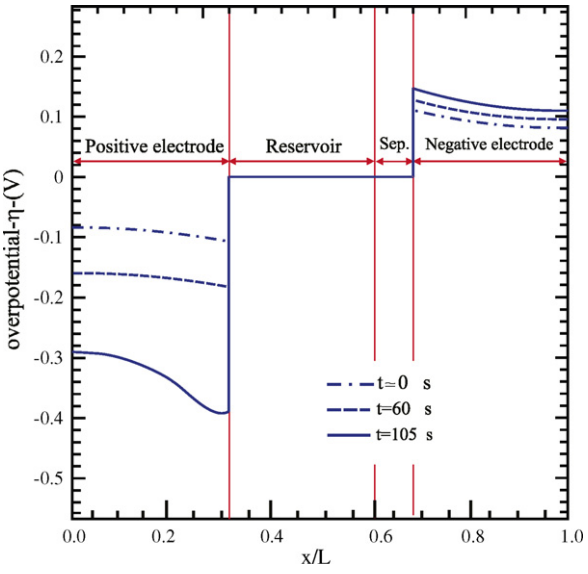

Fig. 10. Distribution of overpotential η across the electrodes during discharge.

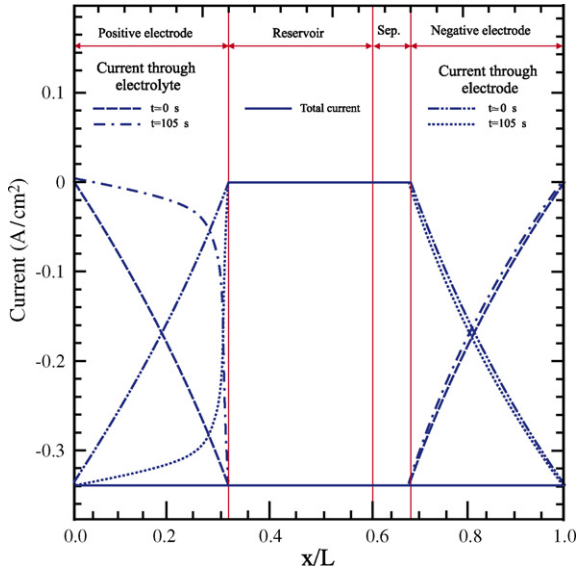

Fig. 11. Distribution of current through the cell.

again in a reverse manner. As it can be seen from the figure at each point through the cell width the summation of i_s and i_l is constant and equals to applied current density. The same behavior is observed during discharge.

Table 1 shows the comparison between computational time of current method with previous CFD simulations. As it can be seen, the present model requires much less computational time in comparison with conventional CFD methods. The speed up factor of the comparison shows that this method accelerates the solution about 50 times. This comparison illustrates the significance of the present model in battery modeling both in real-time simulation and optimization algorithms.

6. Conclusions

In this paper an improved mathematical model for lead-acid batteries based on CFD and ECM has been introduced. This model inherits accuracy of CFD model and physical understanding of ECM. Moreover, it is very fast which makes it quite suitable for real-time simulations. The present model not only predicts battery dynamical characteristics but also is capable to solve distributed parameters such as acid concentration distribution versus time. The present approach is verified by previous CFD models and experimental data. The results show that this model has a good accuracy and the execution time is quite fast enough for real-time purposes and optimization processes.

Acknowledgment

The authors wish to gratefully acknowledge the financial support from Niru Battery Manufacturing Co. and Vehicle, Fuel and Environment Research Institute of the University of Tehran.

References

[1] N. Abolhassani, N. Gharib, H. Moqtaderi, M. Amiri, F. Torabi, A. Mosahebi, M. Hejabi, J. Power Sources 158 (2006) 932–935.
[2] M. Thele, J. Schiffer, E. Karden, E. Surewaard, D.U. Sauer, J. Power Sources 168 (2007) 31–39.
[3] E. Karden, S. Buller, R.W. De Doncker, Electrochim. Acta 47 (2002) 2347–2356.
[4] J. Neumann, W. Tiedmann, AICHE J. 21 (1975) 25.
[5] D.M. Bernardi, H. Gu, A.Y. Schoen, AICHE J. 140 (1993) 2250.
[6] C.Y. Wang, W.B. Gu, J. Electrochem. Soc. 145 (1998) 3407–3417.
[7] H. Gu, T.V. Nguyen, R.E. White, J. Electrochem. Soc. 134 (1987) 2953.
[8] W.B. Gu, C.Y. Wang, B.Y. Liaw, J. Electrochem. Soc. 144 (1997) 2053.
[9] V. Esfahanian, F. Torabi, J. Power Sources 158 (2006) 949–952.
[10] B. Schweighofer, B. Brandstatter, Int. J. Comput. Math. Electrical Electron. Eng. 22 (2003) 703.
[11] V. Esfahanian, F. Torabi, A. Khajavi-Rad, Proceedings of the 10th European Lead Battery Conference, Athens, September 26–29, 2006.